

RHEINISCHE FRIEDRICH-WILHELMS-UNIVERSITÄT BONN

ADVANCED LABORATORY COURSE

PERFORMED ON: APRIL 4TH - 5TH, 2022

SUBMITTED ON: MAY 3, 2022

---

## A249: Laser Gyroscope

---

*Authors*

Paarth Thakkar  
Keito Watanabe

*Tutor(s)*

Thorsten Groh  
Marc Vöhringer

**Abstract**

# Contents

<b>1</b>	<b>Introduction</b>	<b>2</b>
<b>2</b>	<b>Theory</b>	<b>3</b>
2.1	Gyroscopes . . . . .	3
2.1.1	The Sagnac Effect . . . . .	3
2.1.2	Ring Laser Gyroscopes . . . . .	4
2.2	Optical Cavities . . . . .	5
2.2.1	Finesse . . . . .	5
2.2.2	Lock-In Effect . . . . .	5
2.3	Allan Deviation . . . . .	5
<b>3</b>	<b>Pre-Lab Exercises</b>	<b>6</b>
3.1	Task 1: Getting Started . . . . .	6
3.2	Task 2: Allan Deviation . . . . .	6
3.3	Task 3: Rotation Rate of Earth . . . . .	6
<b>4</b>	<b>Experimental Set-Up and Procedure</b>	<b>7</b>
4.1	Experimental Set-Up . . . . .	7
4.2	Procedure . . . . .	7
4.2.1	Free Spectral Range . . . . .	7
4.2.2	PDH Error Signal . . . . .	8
4.2.3	Cavity Ring-Down . . . . .	8
4.2.4	Scale Factor . . . . .	8
4.2.5	Allan Deviation . . . . .	8
<b>5</b>	<b>Results and Discussion</b>	<b>9</b>
<b>6</b>	<b>Conclusion and Outlook</b>	<b>10</b>
<b>7</b>	<b>Acknowledgements</b>	<b>11</b>
<b>8</b>	<b>Appendix</b>	<b>12</b>

## Chapter 1

# Introduction

# Chapter 2

## Theory

### 2.1 Gyroscopes

#### 2.1.1 The Sagnac Effect

The Sagnac effect tells us that whilst the motion between two inertial frames cannot be distinguished, two rotating frames can be distinguished, allowing one to directly measure the rotation rate of an inertial system [1]. This effect was first observed by George Sagnac in 1913, whom believed that this experiment was a proof that aether exists in an inertial frame [2]. This, however, was disproven by Max von Laue in 1911 where he showed that the Sagnac effect was compatible with special relativity [3]. However, the interpretation of the Sagnac effect due to the general theory of relativity is still investigated today, even though it is already well-known in literature [4]. In our analysis, we utilize the Sagnac effect on a gyroscope to measure the rotation rate of the Earth.

To observe the Sagnac effect, we consider an interferometer setup with light propagating with wavelength  $\lambda$  enclosing an area  $\vec{A}$  with perimeter  $P$ . Placing such a setup onto a rotating platform with frequency  $\vec{\Omega}$ , we observe that the optical path that each light travels changes. For example, if the table rotates counter-clockwise, then the path of the co-rotating light increases, while that of the other light decreases (see Fig. 2.1.1). The Sagnac effect then tells us the resulting phase shift between the two lights:

$$\delta\phi = \frac{8\pi\vec{A}\cdot\vec{\Omega}}{c\lambda} \propto \vec{A}\cdot\vec{\Omega} \quad (2.1.1)$$

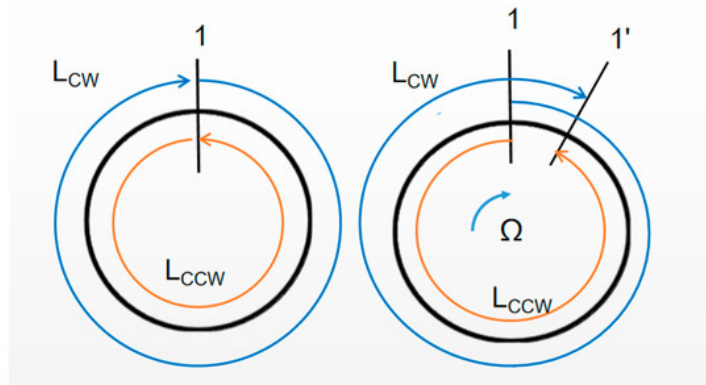


Figure 2.1.1: The Sagnac effect. *Left*: Setup without rotation. The beam moving clockwise (blue) and counter-clockwise (orange) have the same optical path length. *Right*: Setup with a clockwise rotation  $\Omega$ . The path length of the clockwise beam is larger than that of the counter-clockwise beam. Obtained from Ref. [5].

A more detailed derivation using the relativistic law of velocity addition can be found in Ref. [4].

## 2.1.2 Ring Laser Gyroscopes

### Active Ring Laser Gyroscopes

In order to incorporate the Sagnac effect within our experiment, we utilize ring laser gyroscopes. A laser is placed within an enclosed cavity, and emits two counter-propagating beams. Such beams reflect off mirrors and interfere at the end of their propagation. When rotating the platform in which such setup is placed, different interference patterns can be observed, and transforms the ring cavity system into a cavity resonator. The corresponding beat frequency  $\delta\nu$  observed is then the Sagnac frequency, which is given as such:

$$\delta\nu = \frac{4\vec{A} \cdot \vec{\Omega}}{P\lambda} \quad (2.1.2)$$

In our experiment, we only consider square ring cavities so that  $A = L^2$  and  $P = 4L$ , where  $L$  is the path length of each arm. As such, we can simplify Eq. 2.1.2 as such:

$$\delta\nu = \frac{L\Omega}{\lambda} = n\Omega \quad (2.1.3)$$

where  $n = L/\lambda$  is the number of nodes of the light field in each arm. Thus the Sagnac frequency is proportional to the rotation rate of the inertial system [1].

### Passive Ring Laser Gyroscopes

In contrast to the active ring laser gyroscope, in which the laser is contained within the ring cavity, the passive ring laser gyroscope places the laser source outside of the cavity system. In this system, the external laser is locked to the counter-propagating modes of the resonator. By placing the laser outside of the resonator, we can reduce the systematic effects due to the lasing medium and the lock-in effect (see Sec. 2.2.2), and also increase the available light power for the beam. This method, however, also introduces an added complexity of laser locking [1]. See Fig. 2.1.2 for a comparison between the two systems. In our experiment, we use the passive ring laser gyroscope and thus laser locking becomes an importance in our measurements.

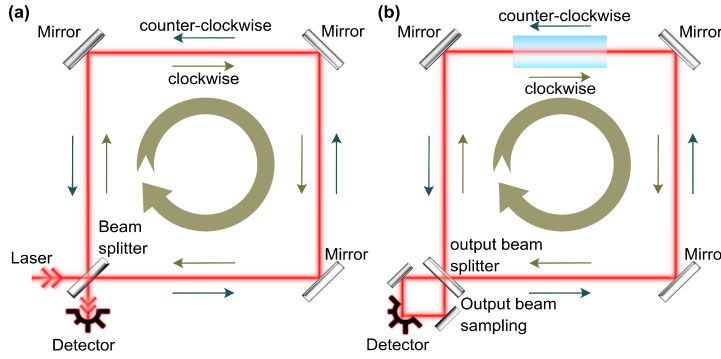


Figure 2.1.2: Ring laser gyroscope systems. *Left: Passive, Right: Active.* Obtained from Ref. [6].

### Gyroscope Sensitivity

The sensitivity of the ring laser gyroscope depends on a variety of factors, namely the wavelength  $\lambda$ , arm length  $L$ , finesse  $F$  of the resonator (see Sec. 2.2.1), and the shot-noise limited detection given by the number of photons  $N = P_{\text{opt}}/h\nu = P_{\text{opt}}\lambda/hc$  detected per unit time.  $P_{\text{opt}}$  represents the optical power given to the laser. Combining all such factors, we obtain the sensitivity of the ring laser gyroscope for an integration time  $\tau$  as such:

$$\delta\Omega = \frac{1}{4} \frac{c}{L^2 F} \sqrt{\frac{ch\lambda}{P_{\text{opt}}}} \frac{1}{\sqrt{\tau}} \quad (2.1.4)$$

This gyroscope sensitivity can be directly compared with the Allan deviation  $\sigma_{\text{ad}}$  that determines the instability of a measurement for some averaged integration time  $\tau$  (see Sec. 2.3). The best gyroscope sensitivity observed was from the G-ring at the German Fundamentalstation Wettzell with a sensitivity of around 12 prad / s /  $\sqrt{\text{Hz}}$  [1].

## 2.2 Optical Cavities

$$\delta\nu_{\text{FSR}} = \frac{c}{P} \quad (2.2.1)$$

### 2.2.1 Finesse

### 2.2.2 Lock-In Effect

## 2.3 Allan Deviation

The Allan deviation is used to quantify the instability of any device that measures differences in frequencies. Assuming that the measurement is only limited by the photon shot-noise (amongst others), we can describe the Allan variance as the deviation between temporal averages of measurements  $y$  over some time interval or integration time  $\tau$ :

$$\sigma_{\text{ad}}^2 = \frac{1}{2M} \sum_{n=1}^M (\bar{y}(\tau)_{n+1} - \bar{y}(\tau)_n)^2 \quad (2.3.1)$$

where  $M$  is the number of samples. The Allan deviation is then the square root of the variance.

The Allan deviation is especially helpful to understand the sensitivity in gyroscopes. Imposing the same assumptions as above, we can describe the Allan deviation with typical shot noise scaling  $\propto 1/\sqrt{\tau}$  as such:

$$\sigma_{\text{ad}} = \frac{\mathcal{A}}{\sqrt{\tau}} \quad (2.3.2)$$

where  $\mathcal{A}$  (given in  $\text{rad/s}/\sqrt{\text{Hz}}$ ) is known as the sensitivity of the gyroscope. This value can be directly compared with the theoretical gyroscope sensitivity described in Eq. 2.1.4 [1].

## Chapter 3

# Pre-Lab Exercises

Before conducting the experiment, we were required to determine the rotation rate of the Earth using our phone. Our phones contain a microelectromechanical system (MEMS), which is a portable and inexpensive inertial sensor that track the motion of the phone. Using the application **phyphox** constructed by RWTH Aachen University, we evaluated the capabilities of the MEMS gyroscope within our phones.

### 3.1 Task 1: Getting Started

### 3.2 Task 2: Allan Deviation

### 3.3 Task 3: Rotation Rate of Earth

## Chapter 4

# Experimental Set-Up and Procedure

### 4.1 Experimental Set-Up

### 4.2 Procedure

#### 4.2.1 Free Spectral Range

We first measured both the signal of the laser input and after the laser has passed through the ring cavity system. The window was adjusted until three resonance peaks and their corresponding sidebands were observed. See Fig. 4.2.1 the observed raw signal.

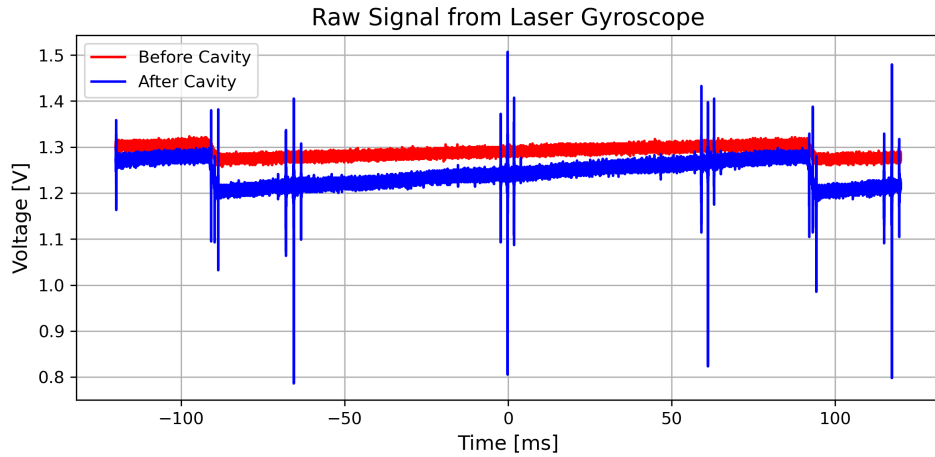


Figure 4.2.1: Raw signal input from the laser before and after passing through the ring cavity system.

As the raw data was provided in the time domain, we converted the time axis into a frequency axis. In order to do so, we use the fact that the modulation frequency from the EOM was  $\Omega = 10$  MHz, and we determined the width in time between the peaks and the sidebands to obtain a conversion factor between the two axes. From this conversion factor, we obtained the free spectral range as the peak-to-peak difference between the resonance peaks. We also took the average of the values to obtain a mean free spectral range.

We then evaluated the cavity perimeter from Eq. 2.2.1 for each free spectral range that we have observed. We compared our obtained results with the measured value of the cavity perimeter  $P_{\text{meas}} = 0.990 \pm 0.005$  m obtained from Ref. [1].



### 4.2.2 PDH Error Signal

### 4.2.3 Cavity Ring-Down

### 4.2.4 Scale Factor

### 4.2.5 Allan Deviation

Finally, we measured the Allan deviation of the laser gyroscope. We performed the same procedure as with the scale factor measurement. Using the same PID parameters as before, we set the rotation frequency to rotate with 0.75 V, so that the laser will remain locked as long as possible. The gyroscope was rotated until the cable connecting the gyroscope did not extend or contract any further, then the same analysis was performed in the opposite rotation direction. The measurement was taken continuously for approximately 1.5 hours. The unprocessed time series for the frequency measurement can be seen in Fig. 4.2.2.

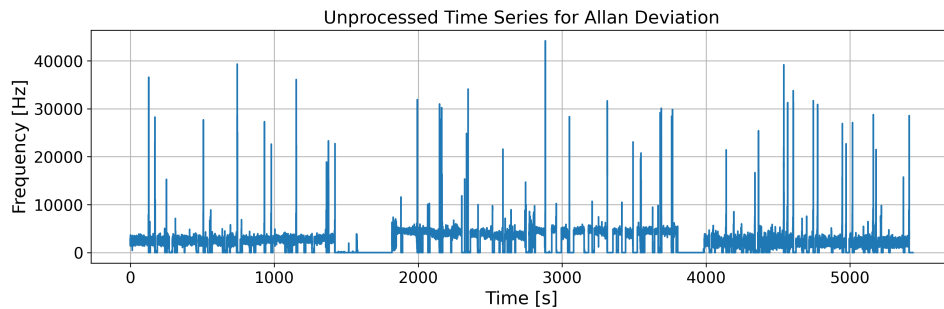


Figure 4.2.2: Unprocessed time series obtained from Allan deviation measurements. We observe large spikes at numerous locations as well as regions with zero frequency.

From the raw data, we first removed any measurements that were taken while the laser was unlocked and when the rotation of the table was switched. After applying some filtering to the data (using `scipy.signal.sosfilt`), we then performed the same procedure as with the Pre-lab tasks in Sec. 3.2 to determine the Allan deviation. We also determined the shot-noise limited time  $\tau$  by observing the time duration in which the instability of the measurement starts. For the rotation frequency of the table, we followed the same procedure from Sec. 4.2.4.

## Chapter 5

# Results and Discussion

## Chapter 6

# Conclusion and Outlook

## Chapter 7

# Acknowledgements

**Chapter 8**

**Appendix**